PHYSICAL REVIEW E **70**, 035204(R) (2004)

Predicting phase synchronization in a spiking chaotic CO_2 laser

Isao Tokuda,[1,2] Jürgen Kurths,[1] Enrico Allaria,[4] Riccardo Meucci,[3] Stefano Boccaletti,[3] and F. Tito Arecchi[3,4]
[1]*Nonlinear Dynamics, Institute of Physics, University of Potsdam, D-14415, Potsdam, Germany*
[2]*Department of Computer Science and Systems Engineering, Muroran Institute of Technology, Muroran, Hokkaido 050-8585, Japan*
[3]*Istituto Nazionale di Ottica Applicata, Largo E. Fermi, 6 I50125 Firenze, Italy*
[4]*Department of Physics, University of Florence, 50019 Firenze, Italy*
(Received 12 May 2004; published 29 September 2004)

An approach is presented for the reconstruction of phase synchronization phenomena in a chaotic CO_2 laser from experimental data. We analyze this laser system in a regime able to phase synchronize with a weak sinusoidal forcing. Our technique recovers the synchronization diagram of the experimental system from only few measurement data sets, thus allowing the prediction of the regime of phase synchronization as well as nonsynchronization in a broad parameter space of forcing frequency and amplitude without further experiments.

DOI: 10.1103/PhysRevE.70.035204 PACS number(s): 05.45.Xt, 05.45.Tp, 52.35.Ra

Synchronization is a fundamental phenomenon of coupled or forced nonlinear oscillators, which is nowadays attracting a significant interest of natural science and engineering. To date, four basic types of synchronization have been found: complete [1,2], generalized [3], phase [4], and lag synchronization [5]. Phase synchronization (PS) of coupled or periodically forced complex systems has found many applications [6], including laboratory experiments, such as circuits [7], lasers [8], plasmas [9], and electrochemical oscillators [10], as well as natural systems, such as cardiorespiratory interaction [11,12], brain activity of Parkinsonian patients [13], paddlefish electrosensitive cells [14], and Canadian lynx-hare populations [15].

To analyze data from such experimental systems, special techniques for PS analysis have been developed and it has been shown that they are very efficient even for noisy and nonstationary data [6,11,13,16]. However, the problem of reconstructing models from such synchronized data remains open. By using such models, it is of special interest to infer a synchronization diagram which yields the regimes of PS, non-PS, and the borderlines between both, which are dependent upon the system parameters, such as the coupling strength and the forcing frequency of interacting nonlinear oscillators. By recovering such synchronization diagram from few sets of experimental data, a deeper insight into the underlying system can be gained. This problem formulation is quite practical in situations where an extensive synchronization experiment is not possible or is very expensive and only limited sets are recorded. To retrieve the synchronization regime, reconstruction of a family of models, which is parametrized by the coupling strength and the forcing frequency, from recording data is required. In a recent study, we introduced a technique for constructing such a parametrized family of coupled nonlinear models based on an artificial neural network and its parameter reduction by singular value decomposition [17]. This approach has the important practical advantage that no prior knowledge of the parametrized family of the dynamics, in particular the underlying system parameter values, is necessary. Our technique has been successfully applied to prototypical PS models and to experimental data from a paced plasma discharge tube, where all of the dynamics were rather phase coherent. However, the technique is not straightforwardly applicable to more complex systems such as fast-slow dynamical systems, which are quite common in nature and engineering. For applications to various natural systems, further extension is required.

The purpose of this paper is to extend this approach [17] to the case of chaotic experimental data from a CO_2 laser [18]. Under certain conditions, the output intensity of the laser consists of a series of spikes with chaotic time intervals [18]. Due to its similarities to electrochemical spike trains traveling on the axons of biological neurons, the laser is considered as a prototypical experimental system for the study of neural activity. With a weak sinusoidal forcing, the laser is able to phase synchronize. The regime of PS gives rise to a clear Arnold tongue structure [8] and, for the experimental parameter used in our measurements, the occurrence of phase slips is characterized by a type I intermittent scaling law [19]. By the extended approach presented here, we demonstrate that the synchronous behavior of the laser system is modeled from only three sets of data, obtained from measurements made with different forcing conditions.

First, we describe the experimental setup and the recording data. Figure 1 shows a single mode CO_2 laser with feedback. The optical cavity, 1.35 m long, is defined by a reflecting grating (M1) acting as a totally reflecting mirror at the desired wavelength (10.6 μm) and a partially reflecting mirror (M2). The laser medium, a gas mixture of CO_2, He, H, and N_2, is excited by a discharge current of 6 mA applied to the laser tube closed by two Brewster windows. The laser cavity also contains an electro-optic modulator which controls the cavity losses by a feedback signal proportional to the laser output intensity. By acting on the two control parameters of the feedback loop, the gain and the bias voltage (B_0), we can set the system in a condition where the output intensity consists of a chaotic sequence of spikes [18] (Fig. 1). The chaotic system can synchronize with an external periodic perturbation applied to the electric discharge [8].

By means of a PC board (NI PCI-6040E) and an acquisition routine on LabView, we constructed the synchronization diagram by applying a sinusoidal perturbation $y(t) = I \sin(2\pi\nu t)$, whose parameters were varied as $(\nu, I) \in [1\ \mathrm{KHz}:2\ \mathrm{KHz}] \times [0\%:3\%]$. Then, for testing and validating our method, the laser intensity $x(t)$ and the external

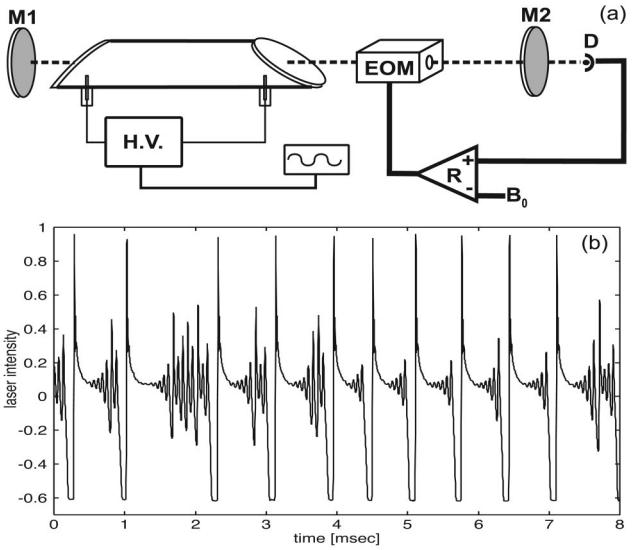

FIG. 1. Experimental setup of the CO_2 laser with feedback (upper) and time series $\{x(t)\}$ of the laser intensity recorded without forcing (lower).

modulation $y(t)$ were simultaneously measured. The data sequences, 10^6 points long, sampled rate $\Delta t=500$ ns with 8 bit vertical resolution were recorded on a digital scope (Lecroy LT 342L) and the acquired intensity data $\xi(t)$ were smoothed by an averaging filter as $x(t)=[1/(20C)]\,\Sigma_{i=0}^{20}\xi(t-i)$ with a normalization constant of $C=0.16$. The recording was made for three different parameter sets $(\nu,I)=(0$ kHz, 0%), (1.1 kHz, 1.5%), (1.7 kHz, 1.5%), which are all in a regime of non-PS. Based on only the three sets of the bivariate data $\{x(t),y(t)\}$, our task is to predict for which parameters of forcing frequency ν and amplitude I the forced system is in the regime of PS.

This condition is practical for experimental situations, where an extensive exploration of the synchronization phenomena is not possible. For instance, in neuroscience, a response characteristic of a single neuron to sinusoidal forcing provides an important clue. Due to its limited lifetime, however, it is almost impossible to investigate the response property of the physiological neuron to every combination of the forcing frequency and the amplitude. It is therefore a strong challenge to estimate the synchronization diagram from only a few sets of recording data.

Figures 1 and 2 show the laser intensity data $x(t)$ and its three-dimensional embedding $(x(t),x(t-10\ \mu\text{s}),x(t-20\ \mu\text{s}))$ recorded from the free running condition where no forcing is applied. The spikes repeat with chaotic time intervals, where the averaged spiking frequency is approximately 1.435 kHz. By the studies based on mathematical models [20], it has been clarified that the spikes are generated by a saddle focus A and a saddle node B shown in Fig. 2. The saddle focus A is composed of a two-dimensional unstable manifold and a one-dimensional stable manifold, whereas the saddle node B has a one-dimensional unstable manifold and two one-dimensional stable manifolds. The typical characteristic of this laser system is its fast-slow dynamical structure. Namely, the laser dynamics is quite slow near the two saddles, whereas it is much faster everywhere else in the phase space.

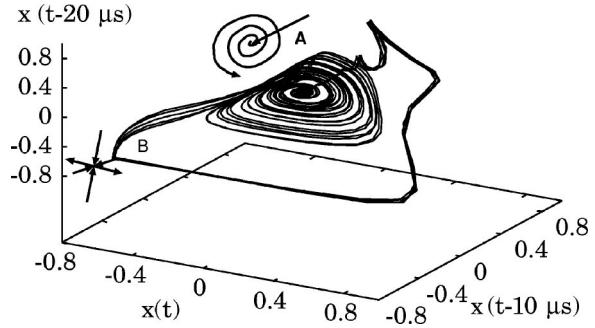

FIG. 2. Three-dimensional embedding $(x(t),x(t-10\ \mu\text{s}),x(t-20\ \mu\text{s}))$ of the laser intensity data of Fig. 1.

Now we describe our modeling technique for the forced system. First, we embed the bivariate time series $\{x(t),y(t)\}$ into delay coordinates $X(t)=\{x(t),x(t-\tau),\ldots,x(t-(d-1)\tau)\}$, $Y(t)=\{y(t),y(t-\tau),\ldots,y(t-(d-1)\tau)\}$ (d is the embedding dimension, τ is the time lag) and suppose according to the embedding theorem [21] that there exists the following dynamics:

$$x(t+1)=F(X(t),Y(t)). \tag{1}$$

The main point of our modeling is to construct a nonlinear function $\tilde{F}$ that approximates Eq. (1). Since the function F is in an input-output form, which requires rather complex modeling, we make a simplification. Namely, according to the property of PS, which is induced by only a small forcing strength, we assume that the intensity of the forcing is much smaller than that of the forced system ($|y|\ll|x|$) and via a first order approximation we obtain

$$x(t+1)=F(X(t))+\alpha_1 I\sin(2\pi\nu t)+\alpha_2 I\cos(2\pi\nu t). \tag{2}$$

Then we model the forced regime with an approximate nonlinear function $\tilde{F}$. If the original forced dynamics is precisely modeled, the regime of PS as well as non-PS in the parameter space of forcing frequency ν and amplitude I can be predicted by studying the model $\tilde{F}$. A practical modeling procedure is to optimize all parameters $\{\Omega,\alpha\}$ of the model function $\tilde{F}$ by minimizing the cost function:

$$E_D(\Omega,\alpha)=\sum_{t,I,\nu}\{x(t+1)-\tilde{F}(\Omega,X(t))-\alpha_1 I\sin(2\pi\nu t)-\alpha_2 I\cos(2\pi\nu t)\}^2. \tag{3}$$

For the construction of the nonlinear models, there are mainly two approaches: local modeling and global modeling. The local approach is to divide the state space into small regions and construct a linear or nonlinear function in each region [22]. The global approach, on the other hand, yields a single nonlinear function that approximates the global dynamics without dividing the space [23,24]. Although the local approach is capable of a precise modeling of the local dynamics, it is not suitable for modeling the global dynamical structure such as bifurcations [24–26], due to its local property. We therefore take a global approach.

The modeling of the system requires a careful treatment because of its fast-slow dynamical property. To recover the global dynamics, a simultaneous modeling of both slow and fast dynamics is indispensable. It is also important to precisely model the local dynamics near the saddles that characterize the system. To deal with this problem, the radial basis function (RBF) [24,26]

$$\tilde{F}(\Omega, X) = \sum_k \Omega_k \ \phi(\sigma_k, \|X - c_k\|) \tag{4}$$

is exploited, where ϕ and c_k stand for the basis function and the centroid and $\|\cdot\|$ denotes the Euclidean norm. Although the RBF is a global approach, it has a local property, which is suitable for the modeling of our delicate dynamics [26].

Our modeling procedure consists of the following main steps.

(1) The embedding dimension d and the time lag τ are chosen. To determine the time lag, commonly used criteria [27] such as the first zero-crossing point of the autocorrelation function or the first local minimum of the mutual entropy are not exploited. The time lag is chosen so that the structure of the two-dimensional unstable manifold of the saddle focus A is fully unfolded. The embedding dimension is set to be three, because the present chaotic regime can be fully modeled [20] by a set of six ordinary differential equations, whose relevant dynamical variables reduce to three in the proximity of the saddle focus A [20].

(2) Due to the fast-slow dynamics, equally sampled data concentrate much more densely near the fixed points than outside. For modeling both the fast and slow dynamics with a good balance, we scatter the data points. First, we define the slow data as $\{X(t): |x(t+\Delta t) - x(t-\Delta t)|/(2\cdot\Delta t) < \Theta_v\}$, where the threshold Θ_v is chosen so that the points near the saddle focus A are separated from the others. All other data are regarded as fast data. Then among the slow data set, a subset of data satisfying $\{\|X(t) - X(s)\| > \Theta_s, \ \forall \ t,s\}$ is extracted. In the same way, a subset of the fast data satisfying $\{\|X(t) - X(s)\| > \Theta_f, \ \forall \ t,s\}$ is extracted.

(3) From both of the fast and the slow data, the same number of centroids $\{c_k\}$ is randomly selected with an addition of noise. The centroids with additive noise, called *chaperons* [26], have been successfully applied to the modeling of similar chaotic dynamics from string data [26].

(4) As a basis function, Gaussian RBF, $\phi(\sigma_k, r) = exp(-r^2/\sigma_k^2)$, with an inhomogeneous variance parameter, $\sigma_k^2 = \min_{i \neq k} \|\mathbf{c}_i - \mathbf{c}_k\|^2$, is used. Due to the fast-slow property, centroids selected in procedure (3) are located not uniformly in the data space. The inhomogeneous parameters are effective for interpolating such nonuniform centroids.

(5) The model parameters $\{\Omega, \alpha\}$ are optimized by the least-square-error algorithm of the cost function $E = E_D + \beta\{\Sigma_k \Omega_k^2 + \Sigma_k \alpha_k^2\}$, where the first term corresponds to the fitting error of Eq. (3) and the second term corresponds to the regularizer [28]. The regularizing constant β is chosen in such a way that a natural frequency of the nonlinear model is close to the one of the original system.

(6) By changing the frequency ν and the amplitude I of the forced model, $x(t+1) = \tilde{F}(X(t)) + \alpha_1 \ I \sin(2\pi\nu t) + \alpha_2 \ I \cos(2\pi\nu t)$, the model frequency $\tilde{\nu}$ is computed by its free running. The model frequency is defined as an inverse of the averaged interspike interval, where the spike is detected by the occurrence of a large output ($x > 0.7$). The synchronization diagram is finally drawn with a relative frequency difference between the model and the forcing as $\Delta\nu = (\tilde{\nu} - \nu)/\nu$.

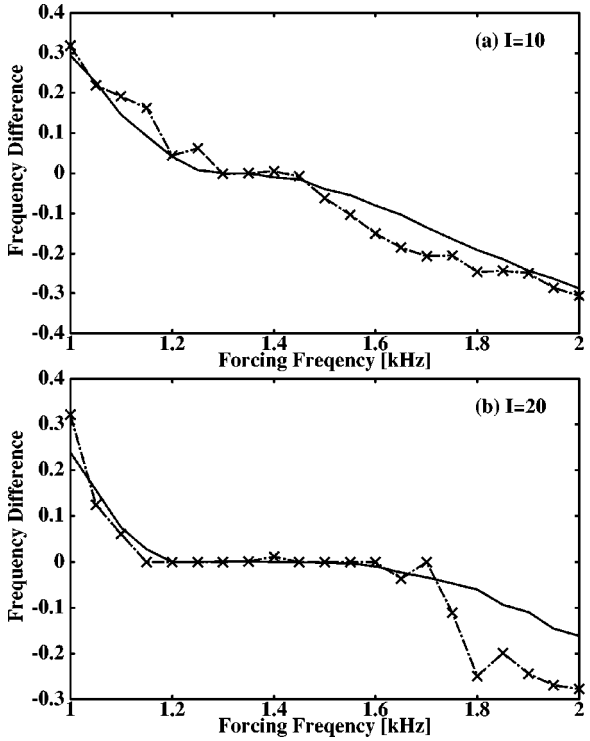

FIG. 3. Relative frequency difference $\Delta\nu$ of the original laser (solid line) and the model (dotted line with crosses) with a varying forcing frequency $\nu \in [1\ \text{kHz}, 2\ \text{kHz}]$ and a fixed amplitude: (a) $I = 1.0\%$, (b) $I = 2.0\%$.

To apply our modeling to the laser experiment, the embedding dimension, the time lag, and the thresholds were set as $(d, \tau, \Theta_v, \Theta_s, \Theta_f) = (3, 10\ \mu\text{s}, 0.0075, 0.012, 0.016)$. From each of the fast and the slow data from a non-forcing experiment, 300 chaperons were randomly selected with an addition of 30% noise of the data. By varying the regularizing parameter in $\beta \in [0.9: 1.1]$, we have confirmed that the nonlinear model yields a natural frequency of $\tilde{\nu} = 1.435$ at $\beta = 1.05$, which coincides in a good accuracy with the laser's original frequency measured from the nonforcing experiment. We therefore exploited the nonlinear model optimized with the regularizing parameter $\beta = 1.05$. Figure 3 gives the synchronization diagrams of the original laser and the nonlinear model in the case when the modulation amplitude is $I = 1.0\%$ and $I = 2.0\%$. The model diagrams show a strong similarity to the original ones. In Fig. 4, borderlines between the regimes of PS and non-PS were drawn for the original laser and the nonlinear model, where the regime of PS was defined as $|\Delta\nu| < 0.05$ [8]. Again the model prediction is in a very good agreement with the experiments. The prediction error in the region of a large forcing amplitude might be due to the limitation of the first order approximation introduced for the nonlinear modeling (2). This demonstrates that by

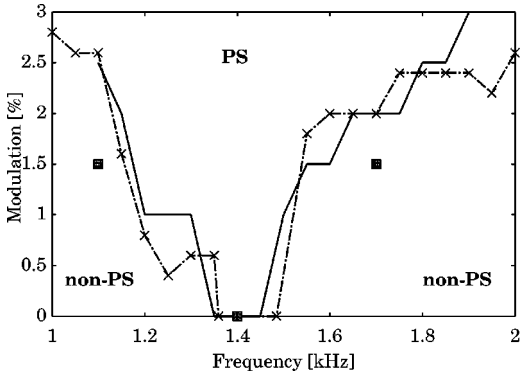

FIG. 4. Borderlines between regimes of PS and non-PS for the laser (solid line) and the model (dotted line with crosses). The three squares indicate locations of the three-recording conditions used for the modeling.

using only three sets of experimental data, synchronization diagram of the chaotic spiking laser can be well reconstructed without further experiments.

To conclude, the modeling approach presented in this paper enables the reconstruction of a synchronization diagram of a forced spiking system from only a few experimental records of bivariate time series. The difficulty of modeling the global properties of such dynamics has been overcome by using the RBF, which is relatively simple to implement. With an application to the experimental data of the CO_2 laser, our technique was capable of predicting the regime of PS as well as non-PS in the parameter space of forcing frequency and amplitude without further experiments. The basic idea of the present approach is general and applicable to other systems. We remark, however, that a certain procedure, e.g., segmentation of the fast-slow data, requires careful inspection of each system. This approach should be of significant importance especially for neuroscientific data, where extensive synchronization analysis in a single neuron is quite difficult due to its short lifetime and reproduction of the same experiment with another neuron is almost impossible. Another important future study is to extend our approach to a network of coupled oscillators, which has many applications to synchronization of spatio-temporal systems such as electrochemical oscillators [10] or brain activity [13].

I.T. was supported by the Alexander von Humboldt Foundation, E.A. was supported by the MIUR-FIRB (No. RBAU01B49F 002), and J.K., R.M., and S.B. were supported by the European project COSYC of SENS (No. HPRN-CT-2000-00158).

[1] H. Fujisaka and T. Yamada, Prog. Theor. Phys. **69**, 32 (1983).
[2] L. M. Pecora and T. L. Carroll, Phys. Rev. Lett. **80**, 2109 (1990).
[3] N. F. Rulkov, M. M. Sushchik, L. S. Tsimring, and H. D. I. Abarbanel, Phys. Rev. E **51**, 980 (1995); L. Kocarev and U. Parlitz, Phys. Rev. Lett. **76**, 1816 (1996); K. Josic, *ibid.* **80**, 3053 (1998).
[4] M. G. Rosenblum, A. S. Pikovsky, and J. Kurths, Phys. Rev. Lett. **76**, 1804 (1996).
[5] M. G. Rosenblum, A. S. Pikovsky, and J. Kurths, Phys. Rev. Lett. **78**, 4193 (1997).
[6] *Phase Synchronization and its Applications*, edited by J. Kurths, special issue of Int. J. Bifurcation Chaos Appl. Sci. Eng. **10**, 2289 (2000); A. Pikovsky, M. Rosenblum, and J. Kurths, *Synchronization—A Universal Concept in Nonlinear Sciences* (Cambridge University Press, Cambridge, 2001); S. Boccaletti *et al.*, Phys. Rep. **366**, 1 (2002).
[7] U. Parlitz, L. Junge, W. Lauterborn, and L. Kocarev, Phys. Rev. E **54**, 2115 (1996).
[8] E. Allaria, F. T. Arecchi, A. DiGarbo, and R. Meucci, Phys. Rev. Lett. **86**, 791 (2001).
[9] C. M. Ticos, E. Rosa, Jr., W. B. Pardo, J. A. Walkenstein, and M. Monti, Phys. Rev. Lett. **85**, 2929 (2000).
[10] W. Wang, I. Z. Kiss, and J. L. Hudson, Phys. Rev. Lett. **86**, 4954 (2001).
[11] C. Schafer, M. G. Rosenblum, J. Kurths, and H.-H. Abel, Nature (London) **392**, 239 (1998).
[12] A. Stefanovska *et al.*, Phys. Rev. Lett. **85**, 4831 (2000).
[13] P. Tass *et al.*, Phys. Rev. Lett. **81**, 3291 (1998).
[14] A. Neiman *et al.*, Phys. Rev. Lett. **82**, 660 (1999).
[15] B. Blasius, A. Huppert, and L. Stone, Nature (London) **399**, 354 (1999).
[16] M. G. Rosenblum, L. Cimponeriu, A. Bezerianos, A. Patzak, and R. Mrowka, Phys. Rev. E **65**, 041909 (2002).
[17] I. Tokuda, J. Kurths, E. Rosa, Jr., Phys. Rev. Lett. **88**, 014101 (2002).
[18] F. T. Arecchi, R. Meucci, and W. Gadomski, Phys. Rev. Lett. **58**, 2205 (1987).
[19] S. Boccaletti, E. Allaria, R. Meucci, and F. T. Arecchi, Phys. Rev. Lett. **89**, 194101 (2002).
[20] A. N. Pisarchik, R. Meucci, and F. T. Arecchi, Eur. Phys. J. D **13**, 385 (2001).
[21] F. Takens, *Dynamical Systems and Turbulence*, edited by D. A. Range and L. S. Young, Lecture Notes in Mathematics Vol. 898 (Springer, Berlin, 1981), p. 366; T. Sauer, J. A. York, and M. Casdagli, J. Stat. Phys. **65**, 579 (1991).
[22] J. D. Farmer and J. J. Sidorowich, Phys. Rev. Lett. **59**, 845 (1987).
[23] J. P. Crutchfield and B. S. McNamara, Complex Syst. **1**, 417 (1987).
[24] M. Casdagli, Physica D **35**, 335 (1989).
[25] R. Tokunaga, S. Kajiwara, and T. Matsumoto, Physica D **79**, 348 (1994); I. Tokuda, S. Kajiwara, R. Tokunaga, and T. Matsumoto, *ibid.* **95**, 380 (1996).
[26] K. Judd and A. I. Mees, Physica D **82**, 426 (1995); **92**, 221 (1996).
[27] H. D.I. Abarbanel, *Analysis of Observed Chaotic Data* (Springer-Verlag, New York, 1996); H. Kantz and T. Schreiber, *Nonlinear Time Series Analysis* (Cambridge University Press, Cambridge, 1997).
[28] K.-R. Müller, S. Mika, G. Rätsch, K. Tsuda, and B. Schölkopf, IEEE Trans. Neural Netw. **2**, 181 (2001).